

# Solid-State Far-Infrared Emitter Utilizing 2D-Plasmon in AlGaAs/GaAs Heterointerface

IN AlGaAs/GaAs HETEROINTERFACE

Noriyuki OKISU, Yasuo SAMBE and Takeshi KOBAYASHI

Faculty of Engineering Science, Osaka University

Toyonaka, Osaka, Japan

Far-infrared (FIR) emission from the grating coupled two-dimensional (2D) plasmon in AlGaAs/GaAs heterointerface was investigated and pretty high emission power of  $30 \mu\text{W}/\text{cm}^2$  ( $460 \mu\text{m}$  wave length) was obtained under the electric field application of  $760 \text{V}/\text{cm}$ . This output power is three orders of magnitude higher than that reported so far. Our calculation suggested that the field application of  $2\sim 3 \text{ kV}/\text{cm}$  is sufficient to offer the radiant FIR ( $100\sim 200 \mu\text{m}$ ) emission in excess of  $\text{mW}/\text{cm}^2$ .

## 1. Introduction

A grating coupled two-dimensional (2D) plasmon at and very near the semiconductor surface is a promising candidate for a tunable solid-state far-infrared (FIR) emitter. The injection type light emitter serves as an efficient photon radiator in the visible and near IR range. However, it becomes out of favor for use in the IR and FIR range because of the dominant non-radiative Auger recombination of the injected minority carriers in semiconductors with very narrow energy gap. Whereas, the plasmon in the semiconductor, an elemental excitation, does not take any special limitation in its oscillation frequency. Moreover, it can be excited simply via the energy and momentum relaxation of the streaming hot electrons and extracted outward by the coupling with a metal grating placed adjacent to the semiconductor surface.

Until now, the experiments have been carried out with Si metal-oxide-semiconductor (MOS) structure<sup>1,2)</sup>, where 2D electrons were induced under the applied gate bias and the plasmon photon came out attenuatively through the thin metal gate. Therefore, the observed FIR emission power was as low as  $10^{-8} \text{W}/\text{cm}^2$  ( $280 \mu\text{m}$ )<sup>2)</sup>. Recent progress of the selectively-doping epitaxial technique has made feasible to

employ  $n^+$ -AlGaAs/GaAs single heterostructures, instead of Si-MOS, to the suitable materials for the plasmon emitter<sup>3,4)</sup>. The other point to be noticed is that establishment of higher electron temperature  $T_e$  is an essential way to grow up the plasmon FIR emission power, since 2D plasmons are excited in energy relaxation process of 2D hot electrons, which are heated up by the applied electric field. Experiments were, however, made only in the low field region<sup>1,2)</sup>. This seems to be the second reason for the observed low emission power stated above. Our previous work was also the case. In the present paper, we report first observation of the plasmon FIR emission and 2D electron temperature under high electric field with AlGaAs/GaAs single interface heterostructure.

## 2. Experimental

### 2-1 Sample preparation and measurement way

The FIR emitters were fabricated on MBE grown heterostructure wafers, the details of which are summarized in Tab. I. The donor impurity in  $n^+$ -AlGaAs layer was Si. The emitter structure shown in Fig. 1 is the same that reported in the last conference. The Au-Ge alloy, rather than AuGeNi, provided better ohmic

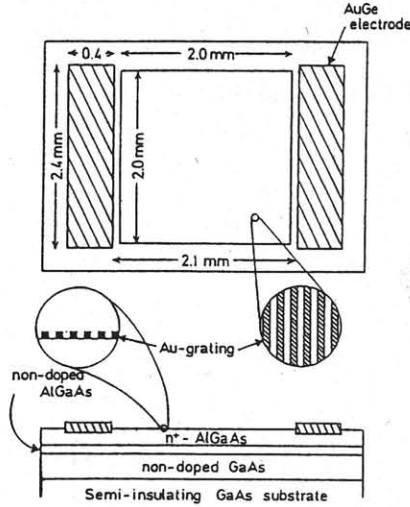


Fig. 1. A top and cut-away view of the completed emitter. Test specimen #60-10. #124-03 has a cap layer on the  $n^+$ -AlGaAs layer.

contact to  $n^+$ -AlGaAs layer even at the cryogenic ambient temperatures.

The metal gratings placed on the top of the epitaxial wafers and between the two electrodes were designed according to the following dispersion relation so as to match the resonant plasmon FIR frequency with the highly pure ( $7 \times 10^{14}/\text{cm}^3$ ) GaAs photodetector detection peak ( $35.5 \text{ cm}^{-1}$ ).

$$\omega^2 = \frac{n_s e^2}{m^*} \frac{k}{\epsilon_{\text{GaAs}} + \epsilon_{\text{AlGaAs}} \tanh(kd_{\text{AlGaAs}})}$$

This simple expression derived in our previous work<sup>5)</sup> is satisfactorily applicable to heterostructures. Prior to the metal-grating formation, thermal FIR measurements were made on all bare emitters to obtain the electron temperature  $T_e$  vs the applied electric field  $E$  relations which facilitate our exploring on the plasmon excitation mechanism, the limitation of FIR

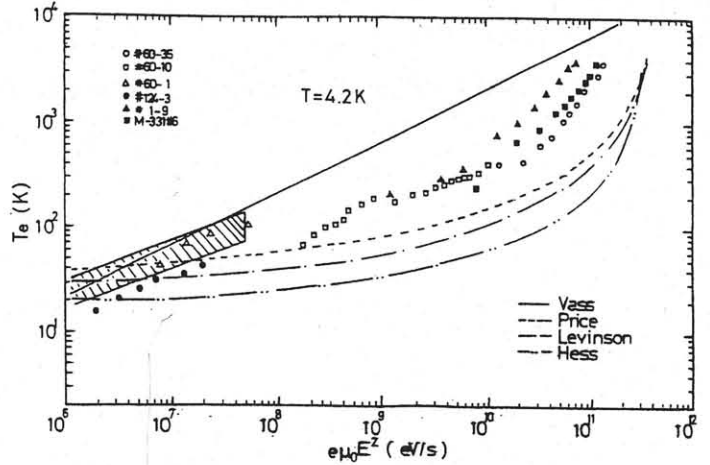


Fig. 2. Electron temperature  $T_e$  vs the input power.  $T_e$  of M-331#6 was measured under the applied field of up to  $10 \text{ kV/cm}$ .

emission power and so on. After this, Au thin films ( $\sim 1000 \text{ \AA}$ ) were deposited onto the AlGaAs surface by resistive heated evaporation and the gratings were patterned with the conventional photolithography and wet etching techniques.

## 2-2. Hot electrons in 2D streams

Throughout the present work, the emphasis is placed on the 2D plasmon excitation under the high electric field. The hot electron behavior in 3D system has been satisfactorily investigated from various aspects. Whereas, the knowledge on hot 2D electrons is still less. This subsection, therefore, denotes to demonstrate how and to what extent the 2D electron temperature is increased by the high field application, and how to save the 2D electrons stream from the real space transfer effect and etc.

The electron temperatures  $T_e$  measured from the thermal FIR power are plotted in Fig. 2 as a function of the input power per an electron

Table I. Device parameters.

Sample type	Layer structure						
	Non-doped	Buffer layer	Doped layer	Cap layer	Surface electron density	Mobility	
	GaAs	$\text{Al}_x\text{Ga}_{1-x}\text{As}$	$\text{Al}_x\text{Ga}_{1-x}\text{As}$	$\text{Al}_x\text{Ga}_{1-x}\text{As}$	$n_s$ ( $\text{cm}^{-2}$ )		
	( $\mu\text{m}$ )	x, ( $\text{\AA}$ )	x, ( $\text{\AA}$ )	x, ( $\text{\AA}$ )			
#60	1.4	0.28 80	0.28 1700	0	$7.2 \times 10^{11}$	58500	
#124	1.4	0.28 70	0.28 350	0.28 5000	$1.4 \times 10^{12}$	8700	
#1	1.5	0.27 63	0.27 2400	0	$5.1 \times 10^{11}$	80000	
M-329	1.1	0.29 100	0.29 2000	0	$7.3 \times 10^{11}$	96500	
M-331	1.1	0.30 75	0.30 2000	0	$6.8 \times 10^{11}$	76100	
M-337	1.2	0.53 50	0.53 2000	0	$4.7 \times 10^{11}$	27100	

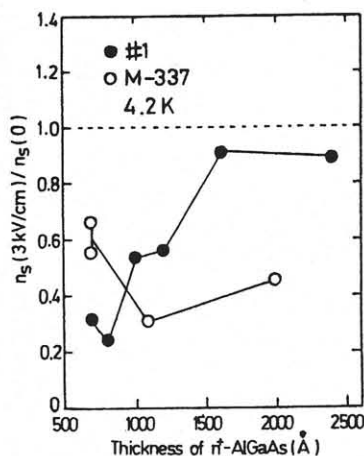


Fig. 3. Reduction of 2D electron concentration via RST vs the thickness of  $n^+$ -AlGaAs layer.

$e\mu_0 E^2$ , where  $\mu_0$  is the field dependent d.c. mobility. The derivation of  $T_e$  can be seen in Ref. 6. This figure clearly illustrates a change of the dominant scattering mechanism as the field intensity increases: Up to  $T_e=100K$ , the acoustic phonon scattering determines the 2D electron transport and  $T_e \propto \sqrt{e\mu_0 E^2}$ . With further increase in  $E$ , the observed  $T_e$  falls on the curve calculated on the dominant polar optical phonon scattering model. As the field intensity increases from 3 to 10 kV/cm,  $T_e$  curve exhibits an steep rise like an occurrence of the polar-runaway and no sign of intervalley-scattering can be found. Anyway, the 2D electron temperature  $T_e$  higher than 3000K can be established under the high field application.

A possible mechanism which deteriorates the stabilized plasmon FIR emission is the real space transfer (RST) of hot electrons. The I-V collapse commonly seen in the so called MODFET is widely known to be due to the RST effect followed by the electron capture at the DX centers in  $n^+$ -AlGaAs layer. A systematic study has been carried to check how strongly the RST effect depends on the energy band diagram of the heterostructure. In Fig. 3, the 2D electron concentration  $n_s$  measured before and after the application of the high field (3kV/cm) are plotted as a function of the thickness of  $n^+$ -AlGaAs layer. Samples fabricated from a wafer #1 ( $x=0.27$ ) give us a simple understanding of the enhanced reduction in  $n_s$  associated with the enlargement of the depletion AlGaAs region adjacent to the heterointerface. The results

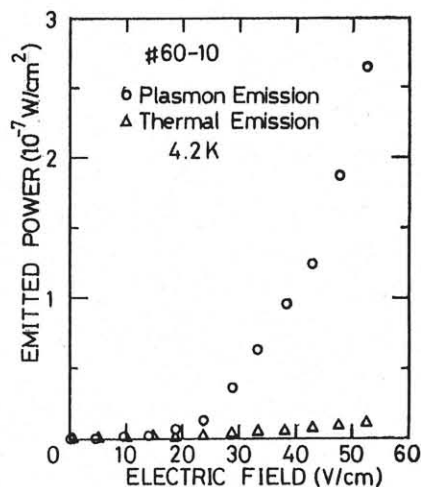


Fig. 4. Plasmon FIR emission power as a function of the applied low field. #60-10.

strongly suggests that the adoption of  $n^+$ -AlGaAs ( $x=0.27$ ) layer thicker than 1500Å is of great favor to establish the stabilization of the high field operation of the plasmon emitter. Though the reason is not known, samples from the wafer M-337 ( $x=0.53$ ) were not up to our expectation regarding the reduced RST effect.

### 2-3. 2D plasmon FIR emission

The grating coupled plasmon FIR emissions were detected even under the applied low electric field, as shown in Fig. 4. In the figure, the thermal FIR power coemitted from the sample is also depicted, being enough low as compared to the plasmon FIR emission. The super-linear increase in the plasmon emission seems to be due to the facts that  $T_e$  increases almost linearly and that the plasmon excitation obeys the Bose-Einstein statistical distribution.

The FIR emission in the high field region is of much interest and the attempt was done in finding the high field 2D plasmon. Figure 5 gives the field dependence of the plasmon FIR emission measured under the applied field ranging from 20 to 760 V/cm, where the RST effect (reduction the 2D electron concentration) was almost completely ignored.

The highest emission power obtained so far was in excess of  $30 \mu W/cm^2$  under the applied field of 760V/cm ( $T_e=400K$ ) at the wave length of 460 $\mu m$ . This value is more than three orders of

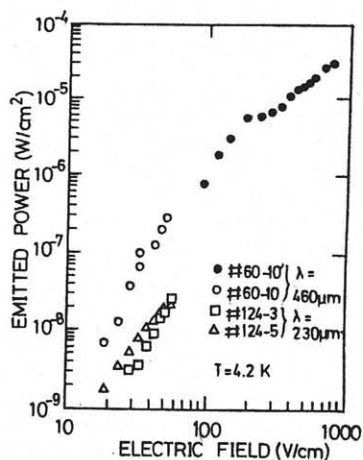


Fig. 5. Measured plasmon FIR emission power vs the applied electric field.

magnitude higher than those ever reported and equivalent to emitted photon number density of  $7 \times 10^{16}/\text{s}/\text{cm}^2$ , which is comparable to the conventional LEDs in IR and visible range. This figure also shows no saturation of emitted power against the applied field. Hence, larger emitted power will be possible to obtain by applying higher field.

Some data of Fig. 5 are reproduced in Fig. 6 with the theoretical curves as a function of the electron temperature  $T_e$ , where the grating antenna coupling efficiency is determined to be 0.01 from the curve fitting.

The experimental data agree with the calculations semiquantitatively. The fact that  $T_e$  in the heterostructures raised up to 4000K when the applied field increased to 3.5kV/cm together with calculations given in Fig. 7 strongly suggest that the FIR emission power necessary for the practical use, order of milli-watts, is promised with our radiator and, besides, it will be able to work even at room temperature.

### 3. Conclusion

The plasmon FIR emission from AlGaAs/GaAs heterostructure was measured under the high field application and the emission power in excess of  $30 \mu\text{W}/\text{cm}^2$  ( $280 \mu\text{m}$ ) was obtained. From the structural improvement, the real space transfer of 2D hot electron and successive trapping at DX centers was avoided to large extent,

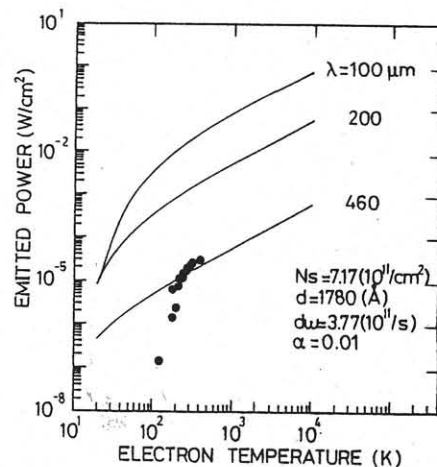


Fig. 6. Calculated plasmon emission power as a function of the electron temperature. Emitter #60. Experimental data of sample #60-10¹ are also shown by solid circles.  $\alpha$  is the grating antenna efficiency.

leading to the stabilized high field operation of the emitter. The electron temperature measurements promised the realization of the radiant plasmon FIR emitter (mW order) in near future.

### Acknowledgments

The authors would like to thank T. Sakurai and T. Tomita of Sharp Corporation for providing MBE grown epitaxial wafers. They also thank T. Shimada for measurement.

### References

- 1) R. A. H8pfel and E. Gornik, Surf. Sci., 1984, **142**, 412.
- 2) R. A. H8pfel, E. Vass and E. Gornik, Phys. Rev. Lett., 1982, **49**, 1667.
- 3) R. H8pfel, G. Lindemann, E. Gornik, G. Stangle, A. C. Gossard and W. Wiegmann, Surf. Sci., 1982, **113**, 118.
- 4) Y. Sambe, N. Okisu, K. Suehiro, T. Kobayashi, K. Fujisawa, T. Tomita and T. Sakurai, Extended Abstracts of the 17th Conference on Solid State Devices and Materials, Tokyo, 1985, 95.
- 5) N. Okisu, Y. Sambe and T. Kobayashi, Appl. Phys. Lett., 1986, **48**, 776.
- 6) R. A. H8pfel, E. Vass and E. Gornik, Solid State Commun., 1984, **49**, 501.